PNAS
www.pnas.org

Supplementary Information for

Methodology and theoretical basis of forward genetic screening for sleep/wakefulness in mice

Chika Miyoshi[1]*, Staci J. Kim[1]*, Takahiro Ezaki[2,3], Aya Ikkyu[1], Noriko Hotta-Hirashima[1], Satomi Kanno[1], Miyo Kakizaki[1], Mana Yamada[1], Shigeharu Wakana[4,5], Masashi Yanagisawa[1,6,7], Hiromasa Funato[1,8]

Correspondence should be addressed to Hiromasa Funato, MD, PhD or Masashi Yanagisawa, MD, PhD.
Email: funato.hiromasa.km@u.tsukuba.ac.jp or yanagisawa.masashi.fu@u.tsukuba.ac.jp

This PDF file includes:

Supplementary text
Materials and Methods
Figs. S1 to S5
Tables S1
Captions for movies S1
References for SI reference citations

Other supplementary materials for this manuscript include the following:

Movies S1

www.pnas.org/cgi/doi/10.1073/pnas.1906774116

Supplementary Information Text

Choice of age and sex of the animals. Screening younger mice can reduce the number of cages used to house mutagenized mice, thus reducing the husbandry and labor cost. However, mice that are too young are vulnerable to implantation surgery, and sleep/wakefulness may not be sufficiently mature. Considering the maturity of the skull and sleep/wakefulness behavior, we performed implantation surgery at 9-10 weeks of age and EEG/EMG recording at 11-12 weeks of age. We used male mice for the strategic advance as the number of sperm from a single male mouse is considerably greater than that of eggs from one female mouse, and sperm can be frozen relatively easily. Also, male mice are preferred in behavioral studies due to the chance of estrous cycle serving as a potential confounding factor, and therefore only a few studies have examined sleep/wakefulness in female mice (1).

Materials and Methods

Animal source and husbandry. C57BL/6J and C57BL/6N mice were obtained from CLEA Japan and Charles River. C57BL/10J mice were from The Jackson Laboratory (#000665). Mice were housed in a polysulfone cage (391 x 199 x 160 mm, floor area 501 cm^2, Techniplast #GM500) in individually ventilated cage racks (Techniplast #DGM70QX) under controlled conditions (12-h light/dark cycle, 23 ± 2°C, 55 ± 5% humidity, and *ad libitum* access to water and food). Mice were weaned at 4 weeks of age and housed in groups of up to 5 mice per cage.

Mutagenesis using ENU. At the age of 8 to 10 weeks, male C57BL/6J mice were treated with ENU (100 mg/kg BW, Sigma-Aldrich #N3385) (2, 3) via intraperitoneal injections three times at weekly intervals following the Mutagenetix protocol (http://mutagenetix.utsouthwestern.edu) (4). The mutagenized mice were housed with wild-type female mice 6-7 weeks after the last ENU injection to check sterility routinely.

In vitro fertilization. Sperms from mutagenized G0 mice were harvested at the age of 25-30 weeks and stored in liquid nitrogen until use. To induce superovulation, adult female C57BL/6N mice were administered with pregnant mare serum gonadotropin followed by human chorionic gonadotropin (hCG) at 48-h intervals. Approximately 15-17 h after hCG treatment, we removed the oviducts from superovulated mice and collected the oocytes. The pooled oocytes obtained from 20 females were inseminated with capacitated sperm. After overnight culture, two-cell stage embryos were transferred into pseudopregnant recipient females. To avoid overrepresentation of the same mutations in sperm differentiated from the same spermatogonia, 60 or fewer F1 males from a single G0 mouse were used for phenotypic screening.

EEG/EMG electrode and tether cable. Each electrode is composed of an insulator (length 7.62 x width 6.08 x height 8.26 mm) with four metal pins (0.50 x 0.40 x 2.6 mm) and two 15-mm-long Teflon-coated stainless wires (Cooner wire #AS633) (Figure S6*A*). The distance between the two metal pins is 5.08 mm in the anteroposterior axis and 2.54 mm in the left-right axis. The Teflon-coat is removed 2 mm from the free end of the EMG wires and soldered using lead-free solder. Four metal pins and EMG wires are gold-plated by immersing them in Supermex #250 (Metalor

Technologies). A tether cable has a four-core shielded cable (Figure S6*B*). The two metal pins on the left side are used to obtain the EEG signal. The one end connected to an electrode is composed of a 6-pin header, which is dissected from 2 x 40 pin header (Useconn Electronics Ltd., #PH-2x40SG) and covered with epoxy resin (Cemedine, High Super 30 #CA-193) or a heat-shrinkable tube (5 mm in diameter, black; Sumitomo Electric, SUMITUBE® C). The other end of the tether cable is composed of a slip ring (yosoo #yosoo-811-3, diameter 12.5mm) or cord detangler (Phillips #SJA4150/17), which allow a mouse to move freely in a recording cage. The tether cable is connected to a cable via 4-pin RJ11 connector, which is subsequently connected to a preamplifier (Figure S6*C*).

EEG/EMG electrode implantation surgery. Eight- to ten-week-old mice (usually heavier than 25 g body weight) were subjected to EEG/EMG electrode implantation surgery. The surgery was performed under isoflurane anesthesia (4% for induction, 2% for maintenance). The scalp was incised along the midline to expose the cranium. Four holes were generated on the skull using 1.0-mm drill bits (anteroposterior: 0.50 mm, lateral: ±1.27 mm and anteroposterior: −4.53 mm, lateral: ±1.27 mm from bregma). The four electrode pins were lowered onto the dura under stereotaxic control (David Kopf Instruments #940/926) and fixed using dental cement (3M ESPE, Ketac Cem Aplicap). Subsequently, two EMG wires were crossed once, inserted into the neck extensor muscles and covered with dental cement. The scalp incision was sutured. A 6-pin header dissected from 2 x 40 pin header (Useconn Electronics Ltd., #PH-2x40SG) was inserted to the top of the EEG/EMG electrode into close the holes of the insulator.

EEG/EMG Recording. Seven days after surgery, the mice were attached to a tether cable under isoflurane anesthesia and after that singly housed in a recording cage (19.1 x 29.2 x 12.7 cm). The tether cable was hung by a counterbalanced lever arm (11.4 cm-long, Instech Laboratories #MCLA) that allows the mice to move freely. All mice were allowed at least 5 days of recovery from surgery and habituation to the recording conditions for at least 4 days. The floor of the cage was covered with aspen chips and nest materials. To examine sleep/wake behavior under baseline conditions, the EEG/EMG signal was recorded for three consecutive days from the onset of the light phase. Mice were deprived of sleep from ZT0 to ZT6 by intermittent mechanical agitation of the cages (5) and subsequently recorded from ZT6 to ZT24 for 18 h.

EEG/EMG analysis. EEG/EMG signals were amplified, filtered (EEG: 0.5–100 Hz; EMG: 0.5–300 Hz) with a multi-channel amplifier (NIHON KODEN, #AB-611J), and digitized at a sampling rate of 250 Hz using an analogue-to-digital converter (National Instruments #PCI-6220) with LabVIEW software (National Instrument). The EEG/EMG data were visualized and semi-automatically analyzed by MATLAB-based software followed by visual inspection. Each 20-sec epoch was staged into wakefulness, NREM sleep and REM sleep. Wakefulness was scored based on the presence of low amplitude, fast EEG activity and high amplitude, variable EMG activity. NREM sleep was characterized by high amplitude, delta (1–4 Hz)-frequency EEG waves and a low EMG tonus, whereas REM sleep was staged based on theta (6–9 Hz)-dominant EEG oscillations and EMG atonia. The total time spent in wakefulness, NREM sleep, and REM sleep were derived by summing the total number of 20-s epochs in each state. Mean episode durations were determined by dividing the total time spent in each state by the number of episodes of that state. Epochs that contained movement artifacts were included in the state totals but excluded from the subsequent spectral analysis. EEG signals were subjected to fast Fourier transform analysis from 1 to 30 Hz with 1-Hz bins using MATLAB-based custom software. The EEG power density in each frequency bin was normalized to the sum of 16-30 Hz in all sleep/wake state.

Linkage analysis using SNPs between C57BL/6J and C57BL/6N. We sequenced SNPs of C57BL/6JJcl, C57BL/6NJcl, C57BL/6NCrl, and C57BL/6NCrlCrlj to select 96 SNPs of C57BL/6JJcl that differ from C57BL/6NJcl, C57BL/6NCrl and C57BL/6NCrlCrlj (Table S1) (6). DNA was purified from tails of mice using a Qiagen kit (DNeasy Blood & Tissue Kit, QIAGEN #69504). SNPs between C57BL/6J and C57BL/6N of N2 mice were determined using a custom TaqMan Genotyping assay (Thermo Fisher). QTL analysis was performed using R/qtl software (version 1.42-8; www.rqtl.org) (7).

Whole-exome sequencing. Exome sequencing libraries were prepared with the SeqCap EZ Developer Library kit (MM10 exome, cat# 110624, Roche NimbleGen) from 500 ng of genomic DNA to determine the number of mutations in the mutagenized mice. Sequencing of the multiplexed library using the 151x2 paired-end mode in the NextSeq 500 sequencer (Illumina) was performed by i-Laboratory LLP sequencing service (Tsukuba, Japan). Reads in FASTQ files were imported into the CLC Genomics Workbench (Qiagen), trimmed by 1-base at the 3' end, and mapped to the mm10 mouse reference, which represents the C57BL/6J strain genome. Exome sequencing statistics were calculated to capture the target region definition provided by the SeqCap kit. Variant calls were performed using the Basic Variant Detection tool. Potential variants were filtered against control mouse variants. Nonsynonymous base substitutions and small InDels were identified based on ENSEMBLE transcript annotation.

For the B016 pedigree, whole exomes were captured with SureSelectXT2 Mouse All Exon (Agilent) and processed to a paired-end 2 x 100-bp run on the Illumina HiSeq2000 platform at the University of Texas Southwestern Medical Center, Next Generation Sequencing Core. Reads were mapped to the University of California Santa Cruz mm9 genome reference sequence for C57BL/6J using Burrows-Wheeler Aligner and quality filtered using SAMtools. Cleaned BAM files were used to realign the data and call variants using the Genome Analysis Tool Kit to detect heterozygous mutations.

Genotyping. To detect a single nucleotide change as routine genotyping, we used the dCAPS method in which PCR products are digested by restriction enzymes (8). dCAPS Finder (http://helix.wustl.edu/dcaps/dcaps.html) was used to design the primers.

Expected number of non-overlapped mutations. The expected number of distinct mutations in F1 mice derived from a single G0 mouse, $N_{\text{non-overlapped}}$, is theoretically given by

$$\boldsymbol{N_{\text{non-overlapped}} = N_{\text{sp}}\left[1-\left(1-\frac{1}{N_{\text{sp}}}\right)^{N_{\text{F1}}}\right]} \quad (1)$$

where N_{F1} and N_{sp} denote the number of F1 mice and the number of A_S spermatogonia in the G0 mouse remaining after ENU treatments, respectively. A formal derivation for this equation is as follows.

Let $P(M, N_{\text{F1}})$ the probability of finding M non-overlapping mutations in N_{F1} individuals. $P(M, N_{\text{F1}})$ satisfies the following recursive formula,

$$P(M, N_{\text{F1}}) = P(M, N_{\text{F1}}-1)\frac{M}{N_{\text{sp}}} + P(M-1, N_{\text{F1}}-1)\left(1-\frac{M-1}{N_{\text{sp}}}\right).$$

Thus, the expected number of M, $E[M; N_{\text{F1}}]$ (= $N_{\text{non-overlapped}}$), is written as

$$
\begin{aligned}
E[M; N_{\mathrm{F1}}] &= \sum_{M=1}^{N_{\mathrm{F1}}} MP(M, N_{\mathrm{F1}}) \\
&= \sum_{M=1}^{N_{\mathrm{F1}}} M\left[P(M, N_{\mathrm{F1}}-1)\frac{M}{N_{\mathrm{sp}}} + P(M-1, N_{\mathrm{F1}}-1)\left(1-\frac{M-1}{N_{\mathrm{sp}}}\right)\right] \\
&= E[M; N_{\mathrm{F1}}-1]\left(1-\frac{1}{N_{\mathrm{sp}}}\right)+1.
\end{aligned}
$$

By solving this recursive formula with $E[M; 0] = 0$ and $E[M; 1] = 1$, we obtain Eq. (1). Figure S1 shows $N_{\text{non-overlapped}}$ for $N_{\mathrm{SP}} = 70$ and 70,000.

Simulations. To simulate the LOD score as a function of mean wake time of mutants, we performed Monte Carlo simulations for various population sizes of N2 mice ($N_{\mathrm{N2}} = 60$, 80, and 120). The LOD score was computed based on surrogate data produced from the empirical data (23 control (+/+) mice and 37 mutant (*m*/+) mice) in the following manner. (i) For each group, we sampled $N_{\mathrm{N2}}/2$ individuals from the empirical data uniformly at random allowing duplication. Note that here we set 50% of the population in the surrogate data to be mutants. (ii) The mean wake time of each control mouse was replaced by a random number sampled from a Gaussian with its mean and SD being 740 min and 740 x 0.1 min, respectively, which were determined based on the empirical data. (iii) Similarly, we replaced the data of the mutant group by random numbers sampled from a Gaussian, but its mean and SD (=mean x 0.1) were changed as variables. (iv) For these surrogate data, we computed the LOD score. To compute the LOD score, we used R/qtl package in R (7). We repeated these procedures (i)-(iv) 10,000 times. The average and 95% confidence interval of the LOD score are shown in Fig. S4A and S4B.

We simulated the probability of reaching statistical significance ($P < 0.05$) in the two-sample *t*-test on the mean wake time of 10 control mice and 10 mutant mice. The mean wake time of each individual was randomly determined as described in the previous paragraph. We performed the two-sample *t*-tests for 10,000 sets of randomly generated data. The probability of reaching statistical significance is shown in Fig. S4C.

Statistics. Statistical analysis was performed using SPSS Statistics 22 (IBM) and R software. All data were tested for a Gaussian distribution and variance. We used one-way analysis of variance (ANOVA) followed by Tukey's test to assess sleep parameters of mouse substrains. To assess the reproducibility of the sleep parameters, data from the first and second recordings were analyzed using Pearson's correlation test. $P < 0.05$ was considered statistically significant.

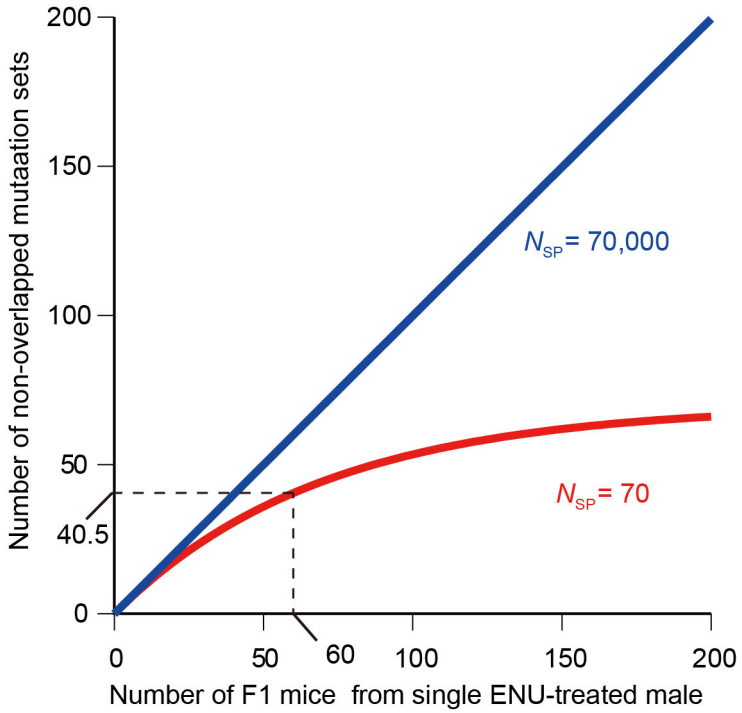

Fig. S1. Number of non-overlapped mutations (Eq. (1)). The expected number of non-overlapped F1 mutant mice derived from a single G0 mouse for N_{sp}=70, when three ENU treatments killed 99.9% of stem-cell-like spermatogonia (red curve). For reference, the results for N_{sp} = 70,000 (when all stem-cell-like spermatogonia in two testes survived the ENU treatments) is shown (blue curve). For example, when the number of screened F1 mice per G0 father was increased from 60 to 90 mice, the number of independent mutant mice increased by approximately 10.

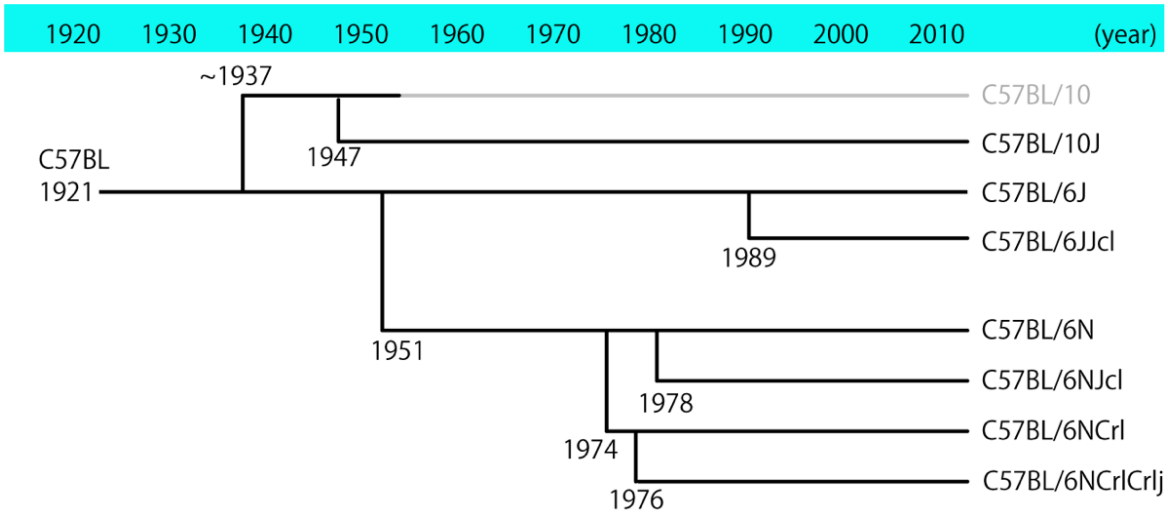

Fig. S2. Phylogenetic tree of C57BL substrains. Abbreviations for the substrain genealogy: N: National Institutes of Health, J: Jackson Laboratory, Crl: Charles River Laboratories, Crlj: Charles River Laboratories Japan, Jcl: CLEA Japan.

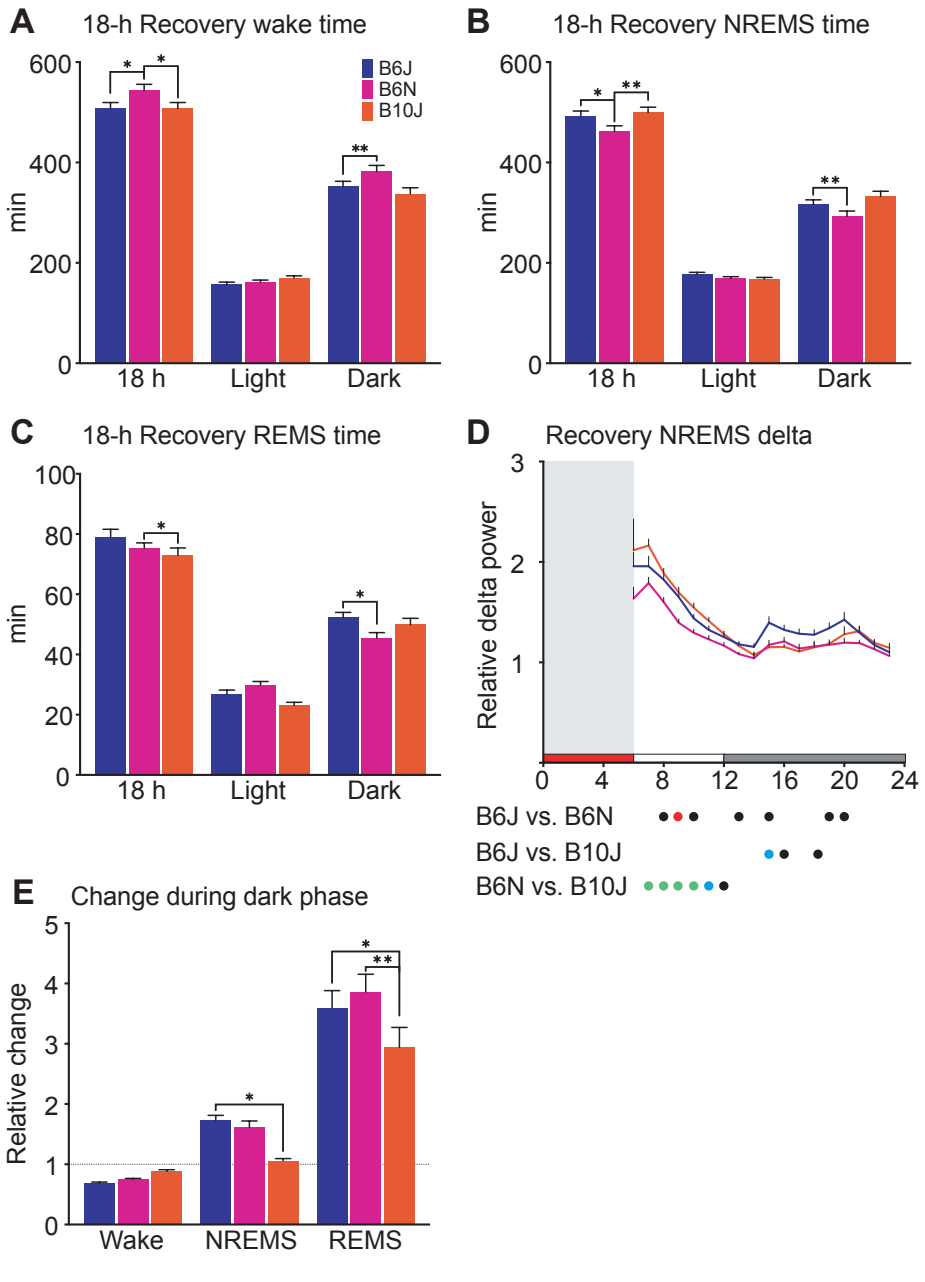

Fig. S3. Recovery sleep after 6-h sleep deprivation. *(A)* Wake, *(B)* NREMS, *(C)* REMS during 18-h recovery following 6-h sleep deprivation. *(D)* NREMS EEG delta during the 18-h recovery. Recovery delta power is normalized by the last hour of the light phase (ZT11) of the baseline. Red-filled box, 6-h sleep deprivation; white box, 6-h recovery sleep; gray-filled box, 12-h dark phase. *(E)* Change, shown as ratio (recovery/baseline), in time spent in each vigilance state during dark phase (ZT12-ZT24). Male B6J (N = 19), B6N (N = 18) and B10J (N = 20). All data are shown as the mean ± SEM *$P < 0.05$; ** (blue) $P < 0.01$; *** (green) $P < 0.001$; **** (red) $P < 0.0001$. Two-way ANOVA followed by Tukey's test.

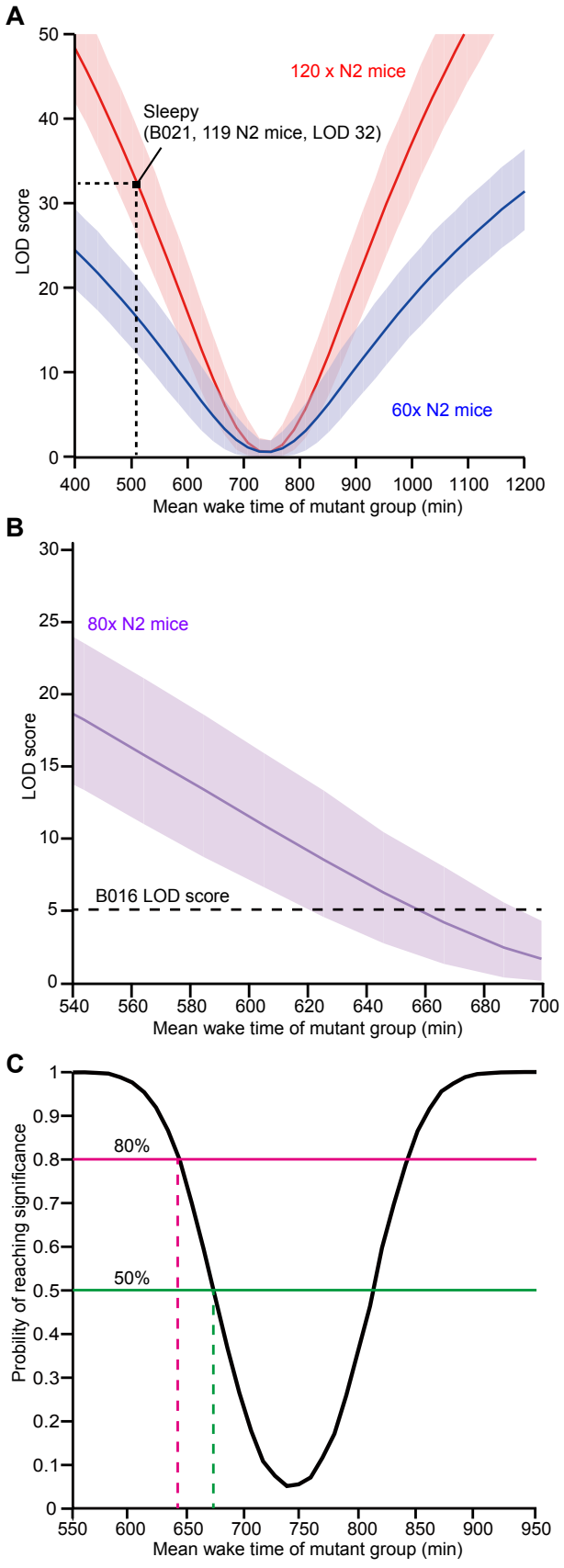
A
120 x N2 mice
Sleepy
(B021, 119 N2 mice, LOD 32)
60x N2 mice
LOD score
Mean wake time of mutant group (min)
B
80x N2 mice
B016 LOD score
LOD score
Mean wake time of mutant group (min)
C
80%
50%
Probility of reaching significance
Mean wake time of mutant group (min)

Fig. S4. Simulation of statistical tests. (*A, B*) The LOD score computed for surrogate data with various mean wake time of the mutant group of 60 (blue), 80 (purple), and 120 (red) N2 mice. The lines and shaded areas indicate the averages and 95% confidence intervals of the obtained LOD score calculated based on 10,000 sets of surrogate data, respectively. In each case, we assumed that 50% of population were mutants. The black square in panel (*A*) indicates the *Sleepy* mutant pedigree, B021. The horizontal dotted line in panel (*B*) indicates the LOD score of 5.17 in the *Drowsy* pedigree, B016 (see Figure 4). (*C*) The probability of reaching statistical significance in a two-sample *t*-test on the mean wake time of 10 control and 10 mutant mice. The results were averaged over 10,000 trials.

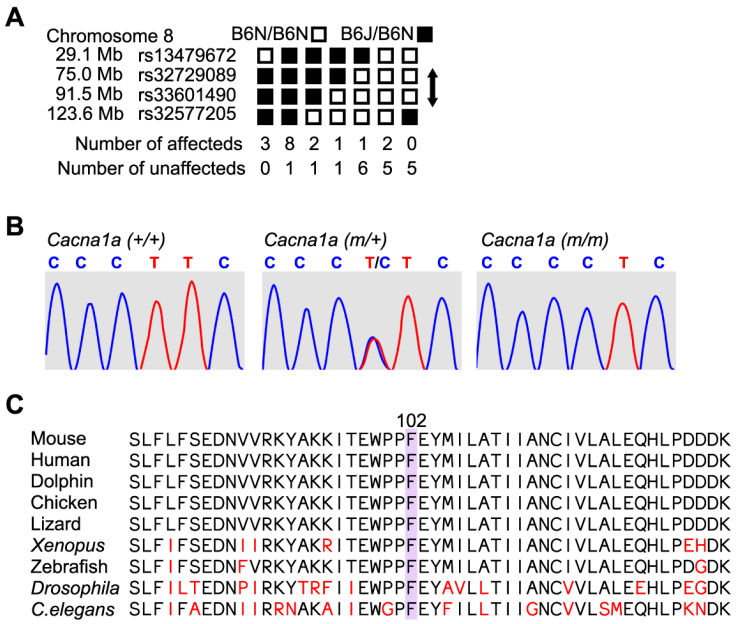

Fig. S5. Identification of the *Cacna1a* gene mutation in the *Drowsy* pedigree. *(A)* Haplotype analysis of affected (bottom 20% in total wake time) and unaffected (top 20% in total wake time) mice within B016 mutant pedigree. Double arrow indicates the chromosomal region of the single LOD score peak above significance threshold. (*B*) Direct sequencing of the *Cacna1a* gene in *Cacna1a*$^{+/+}$, *Cacna1a*$^{m/+}$ and *Cacna1a*$^{m/m}$ mice. (*C*) Phylogenetic conservation around phenylalanine 102

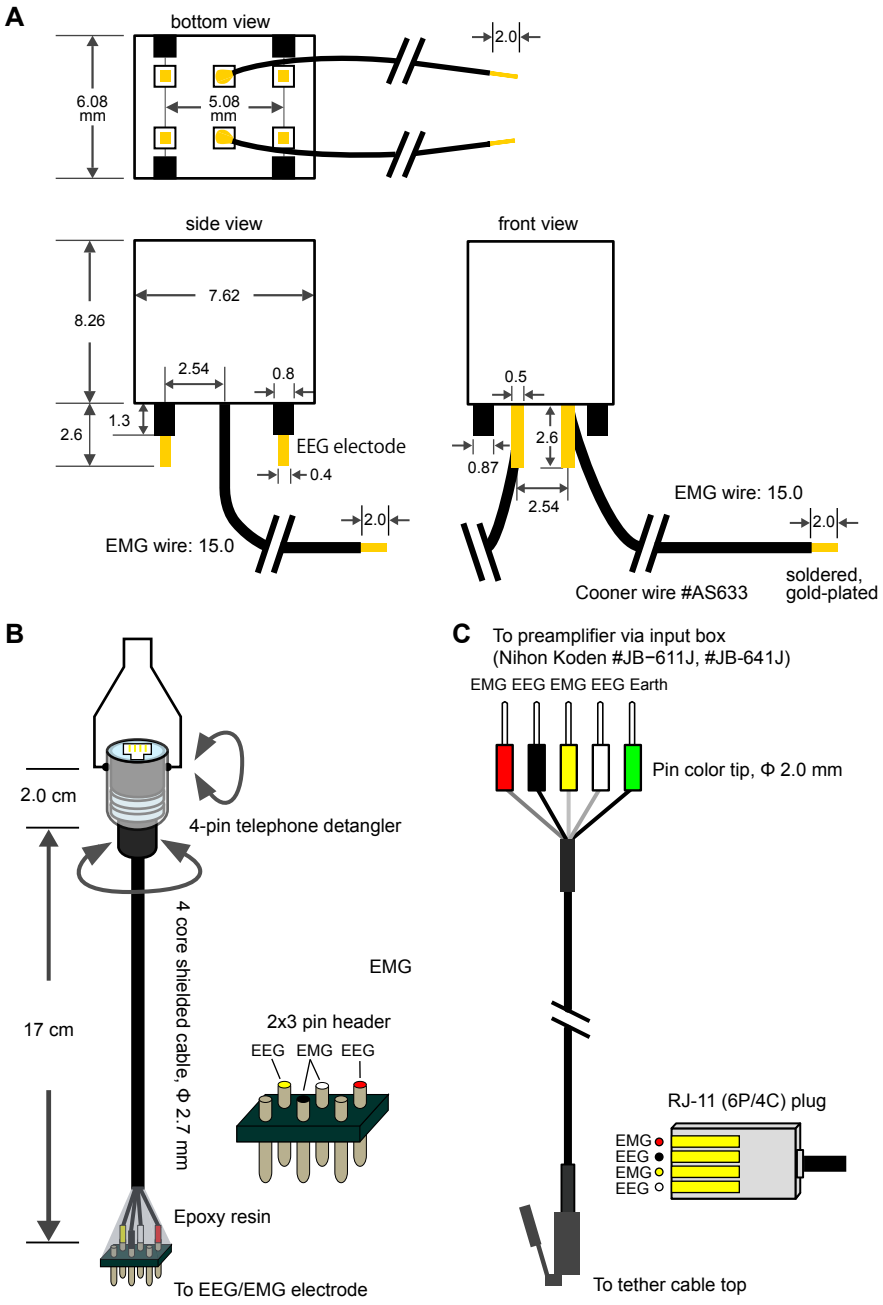

Fig. S6. Design of the electrode and cables. (*A*) Bottom, side and front views of an electrode for EEG and EMG. Four EEG electrodes and one end of two EMG wires are gold-plated. Two of four EEG electrodes are actually used to obtain the EEG signal. Four protrusions close to each EEG electrode enable fixation of the position of an electrode at a certain depth during implantation surgery. The unit for measurements is millimeters. (*B*) A tether cable connects an EEG/EMG electrode and a cable that is connected to a preamp. The top of the tether cable is composed of a 4-pin detangler. (*C*) A cable transmits EEG/EMG signal from the tether cable to a preamp.

Table S1. SNP list for linkage analysis of C57BL/6J and C57BL/6N substrains

Chromosome	Position(mm10)	rs number	B6J	B6N
Chr1	1:3607559	rs32685032	A	T
Chr1	1:42367595	rs31362610	T	C
Chr1	1:88806692	rs242608911	C	T
Chr1	1:129386361	rs6327099	T	C
Chr1	1:163132699	rs6341208	A	T
Chr1	1:194246275	rs242712390	C	A
Chr2	2:8069855	rs13476337	A	T
Chr2	2:45143008	rs33488914	A	G
Chr2	2:78799176	rs33162749	C	T
Chr2	2:106074143	rs227312316	G	A
Chr2	2:138480020	rs13476801	T	C
Chr2	2:179262364	rs29673978	T	C
Chr3	3:5370727	rs13476956	C	T
Chr3	3:27240831	rs237712466	T	G
Chr3	3:54425630	rs31338752	A	G
Chr3	3:74118533	rs31154737	A	T
Chr3	3:107470377	rs31321678	A	G
Chr3	3:152219576	rs31594267	A	C
Chr4	4:6374701	rs32143059	G	A
Chr4	4:28322410	rs13477622	T	C
Chr4	4:65944235	rs13477746	T	C
Chr4	4:110650398	rs245725397	C	T
Chr4	4:132595336	rs46988409	C	A
Chr4	4:155910817	rs6397070	T	C
Chr5	5:4547791	rs247844351	C	T
Chr5	5:40761789	rs33508711	C	T
Chr5	5:70742061	rs13478320	C	A
Chr5	5:92081078	rs33249065	A	G
Chr5	5:117459347	rs3662161	A	G
Chr5	5:149626021	rs33208334	T	C
Chr6	6:6233941	rs30450019	A	G
Chr6	6:44286336	rs30892442	A	C
Chr6	6:80305689	rs48566826	T	A
Chr6	6:117470880	rs13478995	C	G
Chr6	6:141072590	rs235068709	G	T
Chr7	7:6976737	rs242748489	G	A
Chr7	7:37431938	rs31221380	A	C
Chr7	7:71816909	rs32060039	C	G
Chr7	7:104047611	rs46252790	G	A
Chr7	7:129035694	rs13479522	A	G
Chr8	8:10521755	rs13479605	C	A
Chr8	8:29097075	rs13479672	T	C
Chr8	8:56318886	rs32785829	A	G
Chr8	8:91507617	rs33601490	T	C
Chr8	8:123630996	rs32577205	A	G
Chr9	9:6238770	rs33672596	A	G
Chr9	9:31156626	rs13480122	T	C
Chr9	9:52785119	rs29644859	T	G
Chr9	9:85239185	rs260373537	T	C

Chr9	9:119641498	rs30431245	T	C
Chr10	10:5030776	rs50477269	A	G
Chr10	10:33653023	rs13480575	T	C
Chr10	10:57752462	rs13480619	T	C
Chr10	10:80795365	rs13459122	A	T
Chr10	10:109378627	rs13480759	C	T
Chr11	11:4508730	rs3659787	G	A
Chr11	11:21140133	rs29413390	A	G
Chr11	11:48117382	rs13481014	T	C
Chr11	11:79252230	rs13481117	G	T
Chr11	11:120306788	rs49027247	T	C
Chr12	12:7453718	rs29142759	A	G
Chr12	12:34467966	rs29487143	G	C
Chr12	12:62767534	rs29133146	A	C
Chr12	12:85645337	rs13481569	G	A
Chr12	12:106833655	rs13481634	A	C
Chr13	13:18724094	rs29242536	A	G
Chr13	13:41442786	rs3722313	T	C
Chr13	13:77411106	rs29802434	G	C
Chr13	13:101209232	rs3702296	A	G
Chr14	14:9937385	rs31187642	G	A
Chr14	14:36479449	rs31133670	A	G
Chr14	14:74415721	rs30264676	T	A
Chr14	14:99624996	rs31059846	A	G
Chr14	14:124108797	rs31233932	C	T
Chr15	15:9757093	rs257670740	T	C
Chr15	15:30613567	rs261563123	C	T
Chr15	15:71632551	rs31858887	T	C
Chr15	15:97255365	rs31921278	A	G
Chr16	16:4238020	rs4152511	T	C
Chr16	16:32451615	rs257082658	T	G
Chr16	16:52739944	rs4187179	T	C
Chr16	16:87819629	rs4214728	T	C
Chr17	17:5332903	rs4137196	T	C
Chr17	17:39170355	rs33334258	G	A
Chr17	17:60319945	rs13483055	T	C
Chr17	17:93830797	rs33132419	T	C
Chr18	18:15249748	rs13483221	C	T
Chr18	18:35206506	rs13483296	A	T
Chr18	18:54614841	rs13483369	A	C
Chr18	18:84516845	rs29690544	T	C
Chr19	19:9027005	rs31112038	G	C
Chr19	19:21913323	rs45985634	A	T
Chr19	19:38005411	rs30953636	G	T
Chr19	19:49976154	rs3724876	G	T
Chr.20 (X)	X:17562057	rs31353361	T	C
Chr.20 (X)	X:57867627	rs6368704	A	G

Movie S1. B016 (*Cacna1a*) homozygous mutant

Abnormal movement in *Cacna1a* homozygous mutant mice. The mutant mouse did not walk smoothly and frequently fell on its side. The mouse could not control its posture, showed dystonia and slow and clumsy limb movement.

References

1. Komiya H, et al. (2018) Sleep/Wake Behaviors in Mice During Pregnancy and Pregnancy-Associated Hypertensive Mice. *Sleep* 41(3):1–14.
2. Hitotsumachi S, Carpenter DA, Russell WL (1985) Dose-repetition increases the mutagenic effectiveness of N-ethyl-N-nitrosourea in mouse spermatogonia. *Proc Natl Acad Sci* 82(19):6619–6621.
3. Russell WL, et al. (1979) Specific-locus test shows ethylnitrosourea to be the most potent mutagen in the mouse. *Proc Natl Acad Sci* 76(11):5818–5819.
4. Wang T, et al. (2015) Real-time resolution of point mutations that cause phenovariance in mice. *Proc Natl Acad Sci* 112(5):E440–E449.
5. Sinton CM, Kovakkattu D, Friese RS (2009) Validation of a novel method to interrupt sleep in the mouse. *J Neurosci Methods* 184(1):71–78.
6. Kumar V, et al. (2013) C57BL/6N Mutation in Cytoplasmic FMRP interacting protein 2 Regulates Cocaine Response. *Science* 342(6165):1508–1512.
7. Broman KW, Wu H, Sen Ś, Churchill GA (2003) R/qtl: QTL mapping in experimental crosses. *Bioinformatics* 19(7):889–890.
8. Neff MM, Turk E, Kalishman M (2002) Web-based primer design for single nucleotide polymorphism analysis. *Trends Genet* 18(12):613–615.